Enhancing Reinforced Concrete Bridge Health Monitoring: A Case Study on the Integration of InSAR, GPR, and LiDAR within 3D GIS Environment

Ahmed Elseicy[1], Mercedes Solla[1], Jesús Balado[1], Alex Alonso-Díaz[1], Juan Luis Rodríguez[1]

[1] CINTECX, Universidade de Vigo, GeoTECH Group, 36310 Vigo, Spain - {ahmedmossadibrahim.elseicy, merchisolla, jbalado, alex.alonso, jlsomoza}@uvigo.es

Keywords: Infrastructure Health Monitoring, Bridges, LiDAR, GPR, InSAR

Abstract

This work presents a preliminary case study on assessing reinforced concrete pedestrian bridge conditions in A Coruña (Galicia, Spain), employing a novel integration of non-destructive testing (NDT) technologies. The research aims to refine the health monitoring process of pedestrian bridges by adopting a top-down approach, leveraging the data-fusion concept to enhance the analysis of structural defects. A data-fusion methodology that integrates interferometric synthetic aperture radar (InSAR), ground penetrating radar (GPR), and light detection and range (LiDAR) technologies is introduced. Then, the data are visualized within a 3D Geographical Information System (GIS) environment. The MT-InSAR technique is used at the network level to identify bridges requiring detailed inspections. Subsequently, selected bridges undergo thorough examinations using GPR and LiDAR technologies from fieldwork between 2021 and 2023. A comparative analysis of three different LiDAR devices and two GPR setups is conducted to evaluate their effectiveness in capturing detailed structural data. The study also explores the integration challenges and solutions for combining diverse data formats and the possibility of using advanced digital technologies, such as Building Information Modelling (BIM), to facilitate a seamless transition from traditional NDT approaches to a digitized, model-based inspection framework. The findings highlight the advantages of each NDT method, address specific data acquisition challenges, and propose strategies for overcoming issues related to data integration, visualization, and the accuracy of spatial localization. Integrating these NDT technologies within a georeferenced 3D GIS environment facilitates a detailed understanding of the bridge's condition and enhances decision-making processes for maintenance and rehabilitation efforts.

1. Introduction

Bridge inspections are essential to ensure its structural integrity, serviceability, and safety. Moreover, those inspections help to detect defects at early stages and plan the required maintenance and rehabilitation work accordingly. In Spain, bridge inspections are broadly categorized into various types, each serving a specific purpose in assessing the condition and safety of the bridge. These include routine or regular inspections, which are standard visual examinations conducted periodically; major inspections, triggered by specific events or concerns; and special inspections, involving a detailed examination of specific components or conducting loading tests for the formulation of diagnoses (Martí-Vargas et al., 2023). These inspection types reflect a comprehensive and systematic approach to infrastructure management. In addition, each type of inspection contributes to a holistic understanding of a bridge's health and functionality, allowing for targeted maintenance strategies and risk mitigation. Also, the categorization into various inspection types highlights the complexity of the bridge infrastructure management.

In this context, non-destructive testing (NDT) techniques are important in prioritizing bridge management and maintenance within bridge management systems (BMSs) (Akgul, 2020; Elseicy et al., 2022). Multiple NDT techniques can be used at different inspection levels to monitor structures or conduct major inspections (Mugnai et al., 2023). At the network level, interferometric synthetic-aperture radar (InSAR) provides a non-invasive means of inspection, allowing for continuous infrastructure monitoring without the need for physical access to the structure. It can detect surface changes with good precision, offering a high-level detail to monitor structure across the network over time (Tosti et al., 2020). Its capability of continuous monitoring of bridges provides a proactive approach for marking any problems that might arise between periodic inspections or when traditional inspection methods might overlook them (Selvakumaran et al., 2020).

At the project level, integrating LiDAR (Light Detection and Ranging) and Ground Penetrating Radar (GPR) technologies can provide a detailed assessment of the bridge condition for both surface and subsurface (Cafiso et al., 2022). Both technologies are crucial starting from the initial inspection phase or 'state 0'. During this phase, baseline data on the bridge's condition is collected, providing a reference point for subsequent inspections to assess its deterioration rate through its lifetime (Martí-Vargas et al., 2023). However, a key challenge arises from the differing data formats produced by LiDAR and GPR systems from a data integration and visualization perspective. To address this, bridge management systems should act as a unified platform that seamlessly combines the high-resolution point clouds from LiDAR with the subsurface information provided by GPR. Additionally, incorporating detailed visual and structural inspection reports into this platform would create a comprehensive overview of the bridge condition. This integrated approach enhances the accuracy of condition assessments and facilitates more informed decision-making for maintenance and rehabilitation plans.

Modern technologies of digital transition driven by Industry 4.0 are increasingly being adopted as supportive tools within bridge management systems. 3D geoinformation systems can advance spatial analysis and visualization and act as a repository for bridge data. In practical terms, combining maintenance data, CAD drawings and 3D geoinformation acquired by NDT systems can improve the efficiency and accuracy of bridge inspections. Moreover, further processing this information in advanced digital solutions, such as Building Information Modelling (BIM) or digital twins, can transform the user

This contribution has been peer-reviewed. The double-blind peer-review was conducted on the basis of the full paper.
https://doi.org/10.5194/isprs-annals-X-4-W5-2024-155-2024

experience (John Samuel et al., 2022). Accordingly, inspectors can access a wealth of information about the bridge, including its design specifications, historical maintenance records, and real-time data on its current condition. This information can be visualized in a 3D context at the office or on-site through augmented reality, making it easier to identify potential issues and plan effective maintenance strategies.

In this work, three NDT technologies are used to assess the condition of a reinforced concrete (RC) pedestrian bridge in A Coruña (Galicia, Spain). The aim of this case-study is to improve the inspection process of RC pedestrian bridges as a top-down approach. The proposed methodology is based on a data-fusion concept between InSAR, GPR, and LiDAR technologies. The MT-InSAR technique is used at the network level to identify the pedestrian bridges that need closer inspection. Then, a more detailed inspection is performed on a selected bridge using GPR and LiDAR technologies. Three LiDAR devices are used in this case study, and their quality and handling are compared. Moreover, two GPR scans are performed using different setups to assess their suitability for the project. Finally, all the results were visualized within a georeferenced 3D GIS environment. The conclusion of the preliminary study will be further developed towards NDT to BIM approach.

2. The Site and Data Acquisition

2.1 Site description

The structure of this study is a pedestrian bridge in A Coruña, Galicia, Spain, constructed in 1987 (Figure 1a-b), features a unique structural design. It is composed of precast reinforced concrete T-section beams, it includes a central span formed by an isostatic beam with hinged supports at its ends. This central span is joined to cantilever beams, also of the same design, which are mounted on concrete abutments and piles at both sides of the span. Additionally, the bridge incorporates a longitudinal compression layer on the beams, enabling it to function as a continuous beam. To facilitate access, ramps extending from the abutments connect to these beams, integrating seamlessly with the central span.

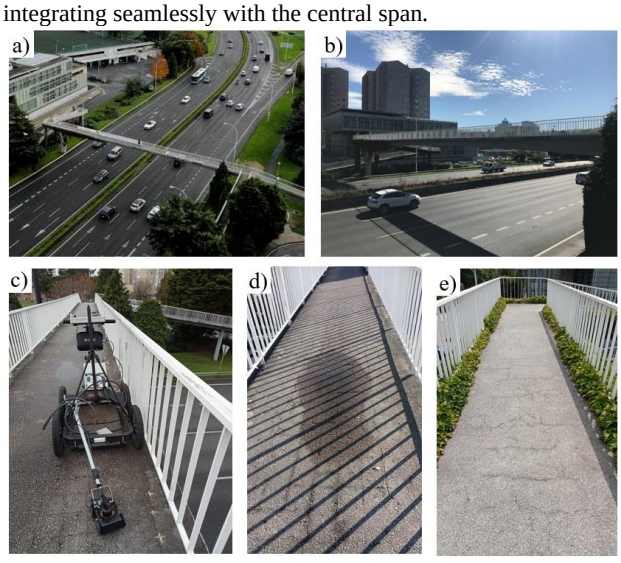

Figure 1. a) Site overview; b) site side view; c) GPR systems; d) water accumulation; e) surface cracks.

Throughout its service life of 37 years, the bridge deck surface suffers from degradation, primarily caused by weather exposure, insufficient maintenance, and consistent pedestrian traffic. Several cracks, stripping, and concrete cover spalling are visible on the surface, exposing the rebars to accumulated rainwater. As a result, this exposure increases the risk of rebar corrosion and material segregation and accelerates the overall damage process. Several control points were marked and taken by GPS in order to georeference both LiDAR and GPR datasets during the post processing step. The GPS system used was a Trimble R8 Model that receives GNSS data from the NAVSTAR and GLONAS constellations, and with precision in differential code positioning of 0.25 meters horizontally and 0.5 meters vertically, and in RTK (Real Time Kinematic) positioning of 10 millimeters horizontally and 20 millimeters vertically.

Figure 2a shows the ground control points taken by GPS at different position in bridge. Moreover, Figure 2b shows a closer look the GPR profile grids taken during the first and second acquisition.

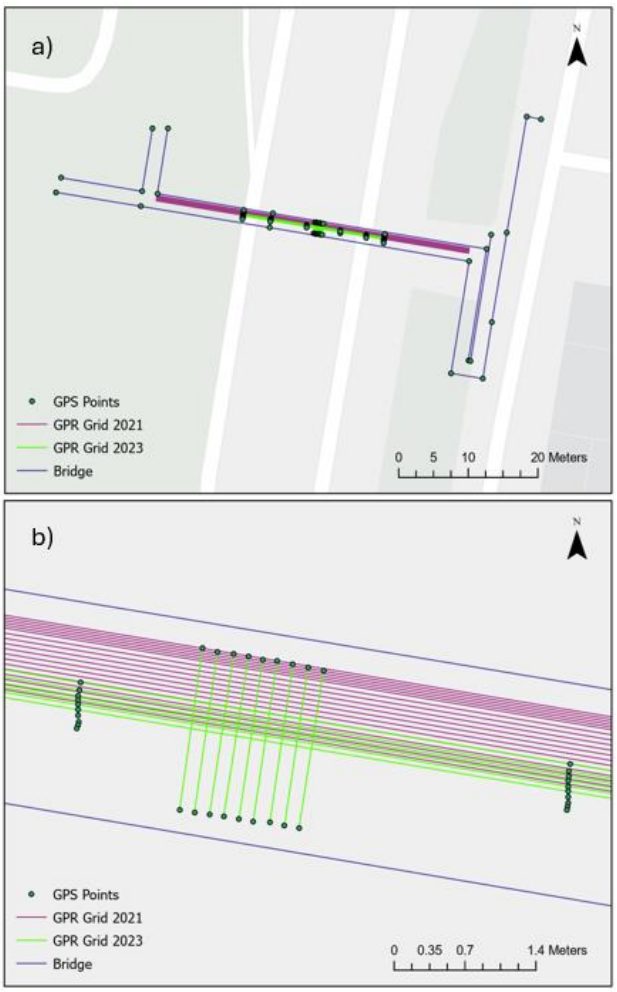

Figure 2. a) Site layout; b) GPR profile grids.

2.2 InSAR

Multi-Temporal Interferometric Synthetic Aperture Radar (MT-InSAR) data were used in this case study to monitor the structure between 09/01/2018 and 18/12/2019. The data were obtained from the Open-access Sentinel-1B satellite constellation. A total of 61 images of ascending orbit and VV+VH polarization were processed. Quasi-PS (QPS) method was implemented with commercial software SARPROZ to

obtain the scatters related to the bridge. Figure 3 illustrates the network of interferograms for the QPS with a total of 850 connections after a coherence threshold of 0.25. After analyzing the scatters influencing the bridge structure, four points of interest have been found (Figure 4a) that show alarming time series (Figure 4b). The four scatters present marking cumulative displacement for the whole period (-89, -10, 11 and 31 mm) and coherence over 0.55.

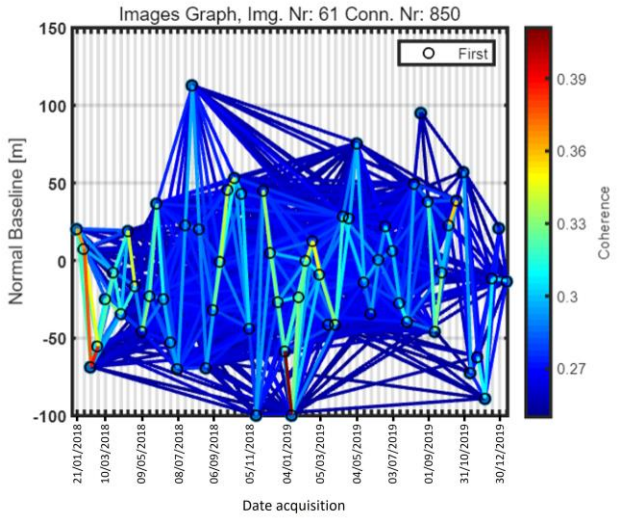

Figure 3. QPS Interferograms network.

Figure 3. a) Scatters location; b) Scatters time-series.

2.3 LiDAR data

In this work, the LiDAR data was acquired to create a detailed 3D point cloud of the bridge. This point cloud is used for visualization in a 3D environment and can be further processed to generate a 3D digital replica of the bridge. Additionally, if the point cloud is dense enough, it can be used to identify surface anomalies such as deformations or cracks. The LiDAR data acquisition was conducted with three different devices to compare their quality and handling.

2.3.1 FARO 3D X330 (Terrestrial Laser Scanner) involved five scans distributed along the platform. One scan was positioned in the center of the platform, two at the ends, and another two in equidistant areas (Figure 4a). Each scan acquisition lasted 6 minutes. The scans were taken in color, although, due to the use of the bridge, many pictures of pedestrians were taken and reprojected on the point cloud, generating false color in digitalized the bridge, so it was finally opted for reflectivity-based color visualization. Although the Faro X330 has an integrated GPS, the accuracy is not enough to obtain a complete consistent point cloud without the need for a later registration. The registration was manually made, taking the central scan position (S1) as a reference. The registration error was 4.1 cm.

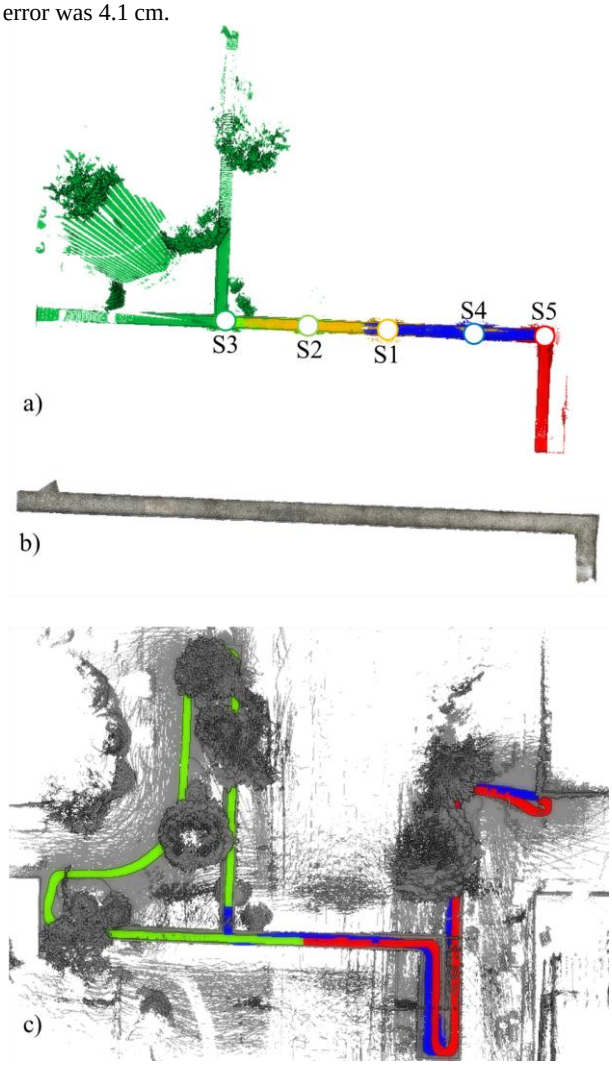

Figure 4. LiDAR data acquisition top view: a) Point cloud from Faro X330 with (S) scan positions, b) Point cloud from iPhone 15 Pro, c) Point cloud from Zeb Go with trajectory (blue-green-red).

2.3.2 iPhone 15 Pro (Low-Cost LiDAR sensor) with *3d Scanner App* was performed following the Faro X330. The iPhone's data acquisition relies on the solid-state LiDAR sensor to capture depth, while the cameras capture color and perform SLAM. The app window allows an augmented reality mesh visualization to be displayed over the bridge as the data is acquired. Even though the bridge was in use during the acquisition, the pedestrian photos were bypassed due to the mobility of the iPhone without apparently affecting the quality

of the final cloud (Figure 4b). The capture with the iPhone for the platform did not require any subsequent registration process.

2.3.3 Zeb Go (Handheld Mobile Mapping System) performed a capture of the complete bridge since a closed loop trajectory is required. To avoid sharp turns in the platform, we chose to follow the trajectory of Figure 4c.
All the point cloud datasets were georeferenced in real-world coordinates using Cloud Compare software using the GPS points.

2.4 GPR Data

GPR works on the principle of emitting high-frequency electromagnetic waves into the ground and recording echoes returning from subsurface structures. Each recorded echo, known as an A-scan, represents a localized point measurement at a specific location, capturing several signal returns over time. These time-domain samples reflect the interaction of electromagnetic waves with the various subsurface materials, allowing the detection of reinforcing bars and changes in material properties or defects. A B-scan is generated by systematically collecting A-scans along a linear trajectory or profile. The B-scan compiles these A-scans side by side to form a continuous cross-sectional image, revealing the subsurface structure beneath the trajectory. This image can be interpreted to distinguish rebars, concrete cover and anomalies with depth based on the time delay and amplitude of the reflected signals.
The collection of parallel profiles across a site allows the assembly of a three-dimensional representation of the subsurface. The 3D GPR dataset, composed of multiple B-scans, provides a volumetric view of subsurface features, improving the interpretation of spatial relationships and the extent of detected features.

Two GPR surveys were conducted (October 7th, 2021, and December 5th, 2023) using different survey wheels (and subsequently different trace spacing or resolution). In both acquisitions, a ProEx system with a high-frequency 2.3 GHz antenna was used. Table 1 shows the specifications of the acquisition. In the 2021 campaign, 18 profile lines (about 48 meters long) were acquired through the longitudinal direction of the bridge, while the GPR survey conducted in 2023 was only applied to the mid-section where the deterioration is more sever. A total of 15 profile lines were acquired, 6 in the longitudinal direction and 9 in the transversal direction (about 20 and 1.6 meters long, respectively). Figure 2 shows the layout of the acquisition grids. It should be mentioned that during the second acquisition, there was accumulated rainwater on the bridge deck which reduced the number of the transversal profiles in the region of interest.

	October 7th 2021	December 5th 2023
Samples per trace	368	432
Central frequency	2.3 GHz	2.3 GHz
Trace interval	8 mm	2 mm
Time window	11 ns	13 ns
Profile line spacing (3D methodology)	2.5 cm / 5 cm	5 cm

Table 1. GPR data acquisitions parameters.

Both GPR datasets were processed using the (*Geolitix | Cloud GPR Processing*, 2024) platform, where the profiles are aligned and georeferenced in a real-world coordinate system based on the acquired GPS points. Then, a set of preprocessing steps were applied to reduce the noise, remove the clutter from the data, and enhance data visualization as the following:

1. A time-zero correction was performed to adjust the starting point of GPR traces to have the correct depth information.
2. A dewow filter was applied to eliminate the low-frequency noise from the data.
3. A bandpass filter was applied to isolate the frequency range of interest, improve the signal-to-noise ratio, and highlight relevant subsurface features.
4. Background subtraction was applied to remove consistent reflections, particularly from the air-concrete interface, thus highlighting the rebars and anomalies representing deterioration within the concrete.
5. A linear gain was applied to compensate for the signal attenuation associated with increased depth and ensure the visibility of deeper structural features.

A bridge deck condition map highlighting the regions with possible defects, such as rebar corrosion, delamination, or moisture damage can be generated from the 3D data by taking horizontal slices with a specific thickness. A basic approach was applied to generate such a map by first normalizing each profile based on its maximum amplitude value. Then, a migration process was applied to correct the hyperbolic responses of the top rebar mat. Finally, the Hilbert Transform was employed for signal envelope detection to facilitate the creation of an accurate and detailed condition map of the concrete bridge deck.

Figure 5 shows an overlay between a condition map for the mid-section of the bridge with a thickness of 5 cm from the deck surface. The red color variation in both maps indicates high envelop values that indicate the damaged areas. Condition maps can be generated with different thicknesses and at different depths and can be also converted to a 3D data cube or point cloud which can be visualsed beside the LiDAR data.

Figure 6 shows several condition maps generated at different depths to see the progression and extent of the damage. Red color can indicate severe damage, detachment, or voids. While Cyan can be small cracks and shallower delamination Blue indicate concrete materials. The strips in the transversal direction in the map highlights the position of the rebars at that depth which can vary in color depending on their amplitude reflection. The velocity used to apply migration was estimated on 12 cm/ns.

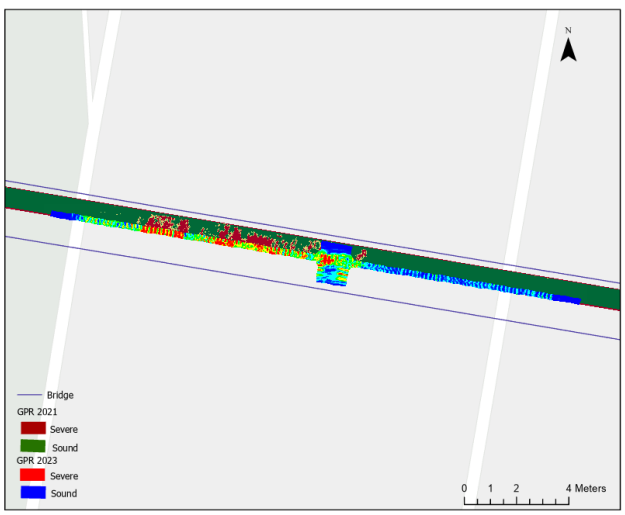

Figure 5. Condition map for the mid-section of the bridge deck from 2021 and 2023 datasets. Color palettes are changed for better visualization.

For accurate representation in 3D, depth correction is applied to the data to compensate for signal velocity variations, which can be affected by the electromagnetic properties of subsurface materials. The correction ensures that the depth of each reflection is accurately located by transforming the raw data into a 3D point cloud. The 3D GPR point cloud can then be visualized with the LiDAR point cloud, providing a complete view of the test site and facilitating detailed analysis and interpretation of the deck conditions. More information cab be then extracted such as concrete cover depth and bridge deck depth which can be useful for generating geometric models. Figure 7 presents an example of the generated 3D data from the parallel profiles and localized under the iPhone dataset. An average velocity of 12 cm/ns was used for depth correction and a basic amplitude outlier detection adopted from (Solla et al., 2022) was applied to highlight the damaged areas.

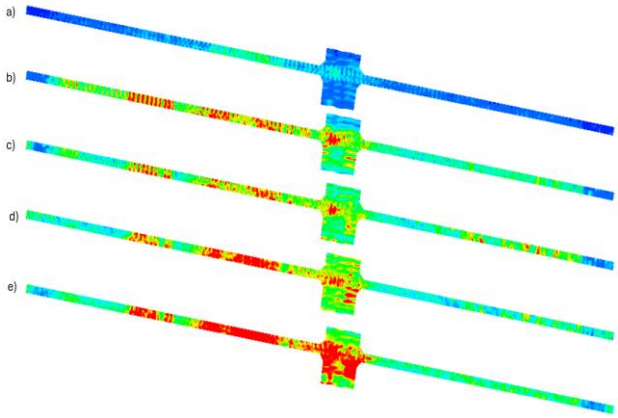

Figure 6. Condition maps for the mid-section of the bridge deck from 2023 datasets. a) at the deck surface; b) at 5 cm depth; c) at 10 cm depth; d) at 15 cm depth; e) at 20 cm depth. Red color refers to areas with potential damage.

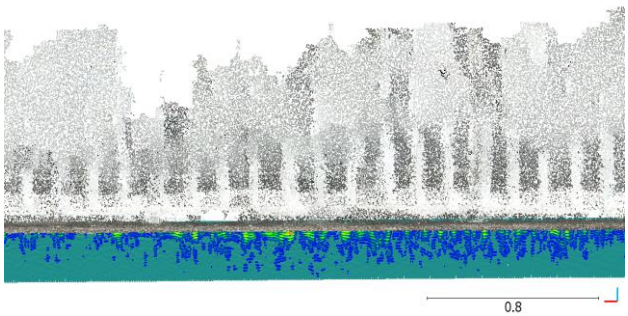

Figure 7. section of iPhone data with the GPR profiles underneath and potential damages are highlighted in Red-Light Green-Blue colors.

3. GIS Data Fusion and Visualization

All the datasets were georeferenced in a common coordinate system, ensuring they were aligned when visualized. The output of the GPR data was a raster image representing the condition of the top 5 cm of the bridge deck. In contrast, the LiDAR data captured the bridge deck in a point cloud format, where each point represents a specific location and elevation on the surface. The ArcGIS platform was used to visualize all the datasets. The platform allows the stakeholders to see the GPR condition maps and LiDAR data in a single view, facilitating a comprehensive understanding of the bridge deck's health. Additionally, the ArcGIS community offers community-based layers, such as 3D cadastral maps or high-resolution imagery, that could be incorporated into the analysis to provide further context. Figures 8-10 illustrate how GPR condition maps can be overlaid on top of the point clouds from various perspectives, offering valuable insights into the bridge deck's condition.

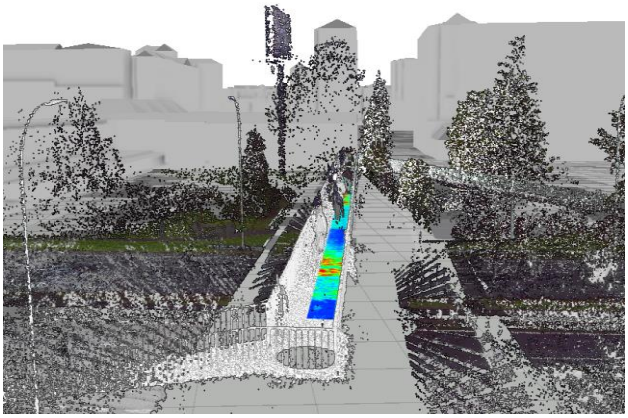

Figure 8. A section of Faro data with an overlay of GPR condition map with 3D cadastre data in the background.

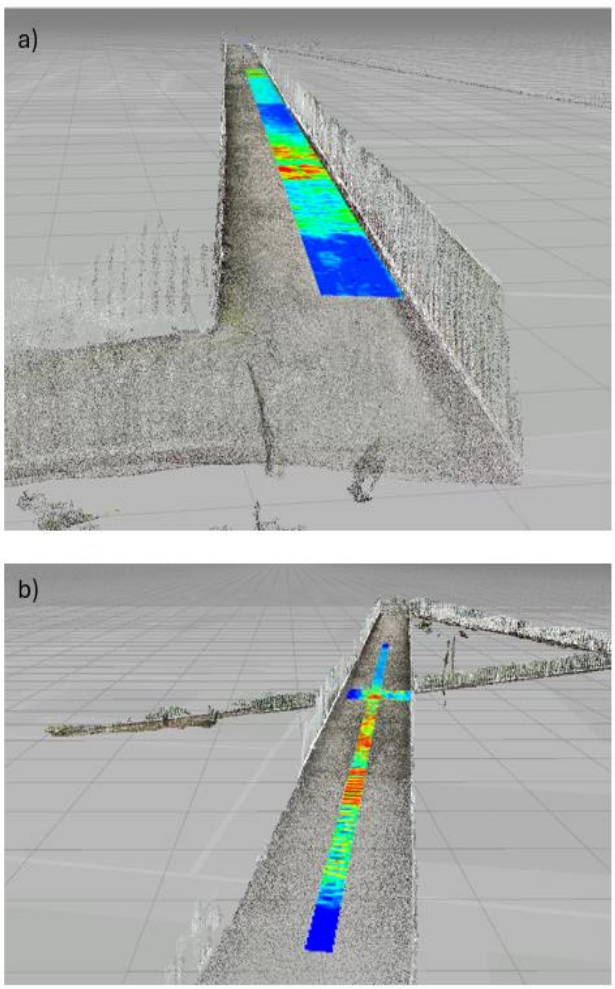

Figure 9. section of iPhone data with an overlay of condition map; a) from 2021 dataset, and b) from 2023 dataset.

This contribution has been peer-reviewed. The double-blind peer-review was conducted on the basis of the full paper.
https://doi.org/10.5194/isprs-annals-X-4-W5-2024-155-2024 | © Author(s) 2024. CC BY 4.0 License.

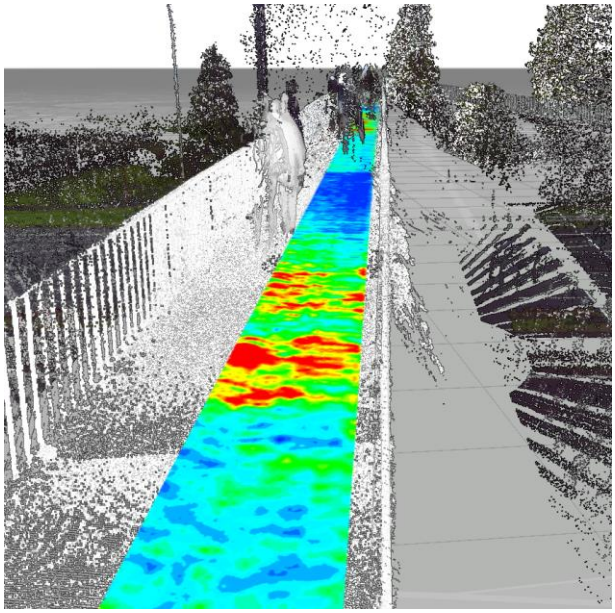

Figure 10. A section of Faro data with an overlay of GPR condition map overlayed on the bridge deck.

4. Challenges and Limitations

The point clouds generated by each sensor have clearly distinguishable characteristics. The Faro point clouds were the most precise and comprehensive, although the data capture and registration took more time. In the Faro point cloud, major cracks and changes in the pavement can be observed, especially based on geometry and reflectivity, but not at the level of detail seen on-site. The point clouds from the iPhone, while showing sufficient RGB colors to identify major cracks, lacked the point density and point quality needed to identify the damaged area of the walkway in detail. The limited geometric quality of the iPhone point cloud is evident in the connection between the railing and the walkway floor, which is a quite diffuse and unrealistic union, unlike the Faro point clouds. In the Zeb Go point cloud, cracks could not be identified. Additionally, the length of the walkway in this point cloud measures 32 meters, while the actual length is 48 meters. This error is attributed to the Zeb Go's exclusively geometric SLAM, which does not perform well in geometrically repetitive environments. In contrast, this problem was not observed in the iPhone as its SLAM is based on imagery.

Several challenges are encountered during data acquisition in the 2021 and 2023 fieldwork. Firstly, site conditions such as deck surface irregularity in the damaged zones can disrupt the contact between the survey wheel and the surface when using small surveying carts. This irregularity impacts the survey wheel's ability to maintain consistent contact with the surface, leading to data loss as the traces are not correctly localized. Therefore, survey marks and field notes should be taken to remove any corrupted or incomplete data. Another issue raised during data acquisition in 2023 was the presence of accumulated rainwater on the bridge deck surface. This issue caused signal attenuation, reducing the radar's ability to effectively penetrate and reflect off subsurface features.

Furthermore, the setup of the GPR system plays a critical role in the success of the survey; improper trace spacing, and profile separation can lead to suboptimal data quality, affecting the detectability of rebar patterns and the identification of small-scale defects such as cracks. For example, the rebar reflection patterns were more distinguishable when using trace spacing of 2 mm in 2023 than when using 8 mm in 2021. However, acquiring more dense data increases the data acquisition time.
Additionally, integrating GPS for spatial localization added more value when integrating data from multiple technologies, but it presents challenges. GPS accuracy is essential for correlating GPR data with precise locations on the bridge deck, especially when using control points linked to survey marks. Moreover, localizing the LiDAR points clouds based on the control points resulted in some inaccuracies due to manual point picking.

Finally, the heterogeneity of data formats poses a challenge in data processing and analysis when visualizing all the results in a 3D GIS environment. Specialized software packages were used to georeference and preprocess the NDT data individually during the preprocessing. Then, the data were exported in common formats such as point clouds, CSV, and images to be ready for further processing. It is essential to work with robust software solutions capable of handling diverse data types while ensuring the integrity and interpretability of the collected information.

5. Conclusions and Future Work

This study presents an approach to monitor the condition of reinforced concrete bridges using NDT technologies. At the network level, InSAR is utilized for broad monitoring purposes, allowing for the prioritization of inspections. LiDAR and GPR are employed for detailed condition assessment. The collected data sets are georeferenced and integrated within a 3D GIS environment. The GIS platform enables the fusion and visualization of data, making it available to stakeholders for enhanced scene understanding and informed decision-making.
While current work presents the GIS approach for data visualization, future work will focus on the bridge management process within digital models. LiDAR data is fundamental in creating detailed as-built digital models of the bridge, identifying surface anomalies, and detecting structural defects. Creating an RGB map (photogrammetry) with surface defects and an Infrared Thermography (IRT) map with shallower defects (such as cracks and delamination up to 2-5 cm deep) can be further optimized for use in augmented reality applications, offering a more immersive analysis experience. GPR technology provides deeper insights into subsurface conditions, including the localization of rebars and detecting various deterioration types. GPR data can be processed into various formats, such as condition maps, localized defect identification, point clouds, or key performance indicators (KPIs), enriching the digital model created from LiDAR data, which will further enhance bridge structures' comprehensive monitoring and management.

Acknowledgements

This work is produced with the support of a 2022 Leonardo Grant for Researchers and Cultural Creators, BBVA Foundation. The BBVA Foundation takes no responsibility for the opinions, statements, and contents of this project, which are entirely the responsibility of its authors. This work has also been supported by the Spanish Ministry of Science and Innovation through the OVERSIGHT project Ref. PID2022-138526OB-I00 funded by MCIN/AEI/10.13039/501100011033/FEDER, UE". A. Elseicy acknowledges the Grant PREP2022-000030 for the training of predoctoral researchers funded by MCIN/AEI /10.13039/501100011033 and by FSE+. M. Solla acknowledges

the Grant RYC2019–026604–I funded by MCIN/AEI/10.13039/501100011033 and by "ESF Investing in your future". J. Balado acknowledges the Grant RYC2022-038100-I funded by MCIN/AEI/10.13039/ 501100011033 and FSE+.

References

Akgul, F. (2020). Inspection and evaluation of a network of concrete bridges based on multiple NDT techniques. *Structure and Infrastructure Engineering*, 1–20. https://doi.org/10.1080/15732479.2020.1790016

Cafiso, S., Di Graziano, A., Goulias, D. G., & Pappalardo, G. (2022). Data Fusion of Non-destructive Testing Methods for Bridge Deck Condition Assessment. *The Open Transportation Journal*, *16*(1). https://doi.org/10.2174/18744478-V16-E221130-2022-15

Elseicy, A., Alonso-Díaz, A., Solla, M., Rasol, M., & Santos-Assunçao, S. (2022). Combined Use of GPR and Other NDTs for Road Pavement Assessment: An Overview. *Remote Sensing*, *14*(17), 4336. https://doi.org/10.3390/rs14174336

Geolitix | Cloud GPR processing. (2024). https://www.geolitix.com/

John Samuel, I., Salem, O., & He, S. (2022). Defect-oriented supportive bridge inspection system featuring building information modeling and augmented reality. *Innovative Infrastructure Solutions*, *7*(4), 1–17. https://doi.org/10.1007/s41062-022-00847-3

Martí-Vargas, J. R., Castro-Bugallo, C., Navarro-Gregori, J., & Mateu-Sánchez, J. A. (2023). Spanish guides and code specifications on concrete bridges inspection and maintenance: an overview. *Ce/Papers*, *6*(5), 833–839. https://doi.org/10.1002/cepa.2111

Mugnai, F., Bonora, V., & Tucci, G. (2023). Integration, harmonization, and processing of geomatic data for bridge health assessment: the Lastra a Signa case study. *Applied Geomatics*, *15*(3), 533–550. https://doi.org/10.1007/s12518-023-00510-1

Selvakumaran, S., Rossi, C., Marinoni, A., Webb, G., Bennetts, J., Barton, E., Plank, S., & Middleton, C. (2020). Combined InSAR and Terrestrial Structural Monitoring of Bridges. *IEEE Transactions on Geoscience and Remote Sensing*, *58*(10), 7141–7153. https://doi.org/10.1109/TGRS.2020.2979961

Solla, M., Buceta-Bruneti, G., Elseicy, A., & Nieto-Muñiz, B. (2022). Ground Penetrating Radar Applied to Monumental Stone Conservation: Application to the Rock Necropolis of San Vítor de Barxacova in NW Spain. *Surveys in Geophysics*, *43*(5), 1587–1606. https://doi.org/10.1007/s10712-022-09728-x

Tosti, F., Gagliardi, V., D'Amico, F., & Alani, A. M. (2020). Transport infrastructure monitoring by data fusion of GPR and SAR imagery information. *Transportation Research Procedia*, *45*, 771–778. https://doi.org/10.1016/j.trpro.2020.02.097